

# Effect of the particle shape on the optical properties of black carbon aggregates

Krzysztof Skorupski

Wroclaw University of Technology, Chair of Electronic and Photonic Metrology,  
Boleslawa Prusa 53/55, 50-317 Wroclaw, Poland

## ABSTRACT

Small particles tend to connect to each other and create large geometries, namely aggregates. To simplify the light scattering simulation process, they are usually modelled as assemblies of spheres positioned in point contact. This is a rough approximation because connections between them always exist. In this work we present answers to the three following questions: which optical properties of fractal-like aggregates are strongly dependent on the particle shape, what is the magnitude of the relative extinction error  $\delta C_{ext}$  when non-spherical particles are modelled as spheres and whether the relative extinction error  $\delta C_{ext}$  is dependent on the aggregate size  $N_p$ . The paper was aimed at tropospheric black carbon particles and their complex refractive index  $m$  was based on the work by Chang and Charalampopoulos. The incident wavelength  $\lambda$  varied from  $\lambda = 300nm$  to  $\lambda = 900nm$ . For the light scattering simulations the ADDA algorithm was used. The polarizability expression was IGT.SO (approximate Integration of Greens Tensor over the dipole) and each particle, regardless of its shape, was composed of ca.  $N_d \approx 1000$  volume elements (dipoles). In the study, fractal-like aggregates consisted of up to  $N_p = 300$  primary particles with the volume equivalent to the volume of a sphere with the radius  $r_p = 15nm$ . The fractal dimension was  $D_f = 1.8$  and the fractal prefactor was  $k_f = 1.3$ . Geometries were generated with the tunable CC (Cluster-Cluster) algorithm proposed by Filippov et al. The results show that when the extinction cross section  $C_{ext}$  is considered, the changes caused by the particle shape, which are especially visible for longer wavelengths  $\lambda$ , cannot be neglected. The most significant difference can be observed for the regular tetrahedron. The relative extinction error  $\delta C_{ext}$  diminishes slightly along with the number of primary particles  $N_p$ . However, even when large fractal-like aggregates are studied, it should not be considered as non-existent. On the contrary, when light scattering diagrams or the asymmetry parameter  $g$  are needed, spherical models can be used, even with relatively small fractal-like aggregates.

**Keywords:** light scattering, discrete dipole approximation, black carbon, soot, fractal-like aggregates

## 1. INTRODUCTION

Soon after emission small particles connect to each other and create more complex geometries, namely aggregates. In spite of the fact that their morphological parameters vary, they reveal fractal-like properties, and therefore, can be described by the following equation:<sup>1,2</sup>

$$N_p = k_f \left( \frac{R_g}{r_p} \right)^{D_f}, \quad (1)$$

in which  $N_p$  stands for the number of primary particles with the radius  $r_p$ . The fractal dimension  $D_f$ , which varies from  $D_f \approx 1$  (e.g. primary particles form a straight line) to  $D_f \approx 3$  (e.g. primary particles form a compact ball), reflects the overall shape of the geometry. The fractal prefactor  $k_f$  is a proportionality constant and  $R_g$  is the radius of gyration. The last parameter can be calculated with the following equation:<sup>3</sup>

$$R_g^2 = \frac{1}{N_p} \sum_{i=1}^{N_p} (\vec{r}_i - \vec{r}_c)^2, \quad (2)$$

---

E-mail: krzysztof.skorupski@pwr.edu.pl

in which  $\vec{r}$  is the position of the  $i$ -th primary particle and  $\vec{r}_c$  is the mass centre of the aggregate. Both equations accurately describe the shape of fractal-like aggregates providing that they are composed of spherical particles positioned in point contact  $C_p = 0$  (i.e. there are no intersections between them).<sup>4</sup> It is not hard to realize that such models are only rough approximations which are commonly used for speeding up the light scattering simulation process.<sup>5</sup> In reality, primary particles are not spherical and advanced connections between them are not rare.<sup>6</sup> The goal of this work was to approximate the optical properties of aggregates composed of much more complex particle models and decide whether they can be used interchangeably with the simplified, spherical one. In this paper black carbon nanoparticles were investigated. They are a product of incomplete combustion of carbon-based fuels, can be hazardous to health and are believed to have an impact on the global warming effect.<sup>7,8</sup> Their complex refractive index  $m$ , which is also in agreement with the criterion proposed by Bond et al.,<sup>9</sup> was adapted from the work by Chang and Charalampopoulos.<sup>10</sup>

All aggregate models used in this study were generated with the FLAGE (Fractal-Like Aggregate Generation Environment) software and the implementation of the CC (Cluster-Cluster) algorithm proposed by Filippov et al. was used.<sup>11-14</sup> The fractal dimension was  $D_f = 1.8$  and the fractal prefactor was assumed to be  $k_f = 1.3$ . The maximum number of primary particles, with the volume  $V = 4/3 \cdot \pi \cdot (15nm)^3$ , was  $N_p = 300$ . They were modelled as: spheres, cubes, tetrahedrons and octahedrons (note, that  $V$  was constant regardless of the particle shape).<sup>8,15,16</sup> Although these are approximate value of investigated morphological parameters of black carbon aggregates, note, that different techniques for measuring them exist.<sup>17-24</sup> Therefore, they may vary across publications. All interactions of generated black carbon aggregates with organic (e.g. acid) and inorganic (e.g. sulphate) matter were neglected.<sup>25</sup> Examples of investigated particle models and generated aggregates are presented in Fig. 1 and Fig. 2 respectively.

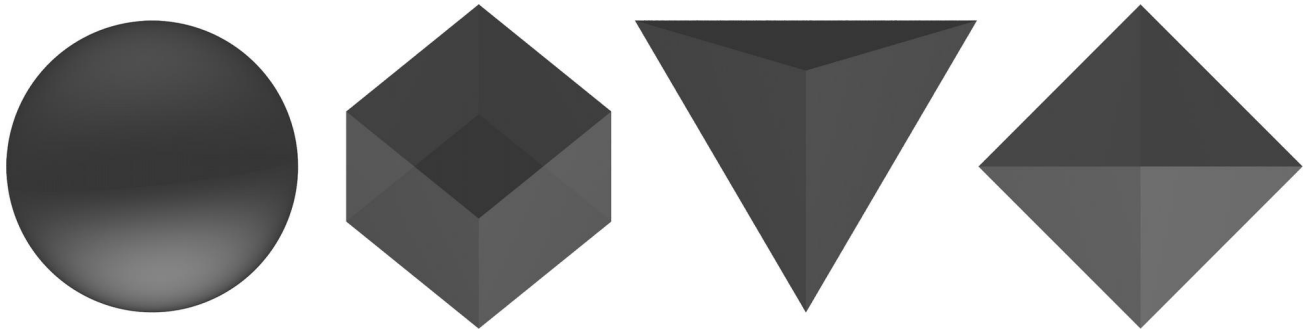


Figure 1: Different primary particle models used in this study. From left to right: sphere, cube, tetrahedron, octahedron.

Light scattering techniques have been commonly used for identifying and measuring various objects, including black carbon aggregates, erythrocytes and fibers.<sup>26-35</sup> In this study the incident wavelength varied from  $\lambda = 300nm$  to  $\lambda = 900nm$  with the step  $\Delta\lambda = 20nm$ . For the light scattering calculations the ADDA algorithm was used.<sup>36,37</sup> The polarizability expression was IGT\_SO (approximate Integration of Greens Tensor over the dipole) and the results for primary particles were averaged orientationally. To reduce the computation time, when large aggregates were studied, only one polarization state was investigated. However, centers of primary particles were always kept in fixed positions, regardless of the particle model used. To guarantee accurate results, every primary particle was decomposed into ca.  $N_d \approx 1000$  volume elements (dipoles) to precisely describe its shape.

## 2. SIMULATION RESULTS - PARTICLES

The absorption cross section  $C_{ext}$  and the scattering cross section  $C_{sca}$  for investigated primary particle models are presented in Fig. 3. Additionally, in Fig. 4 the relative error is shown, i.e.  $\delta C_{abs}$ ,  $\delta C_{sca}$ . The results prove that the particle shape has a significant impact on the absorption cross section  $C_{abs}$ , what is especially visible for long wavelengths  $\lambda$ . The most significant absorption error  $C_{abs}$  was observed for the tetrahedral geometry. This proves that even when the volume of the primary particle  $V$  is conserved, its diameter  $d$  should not be

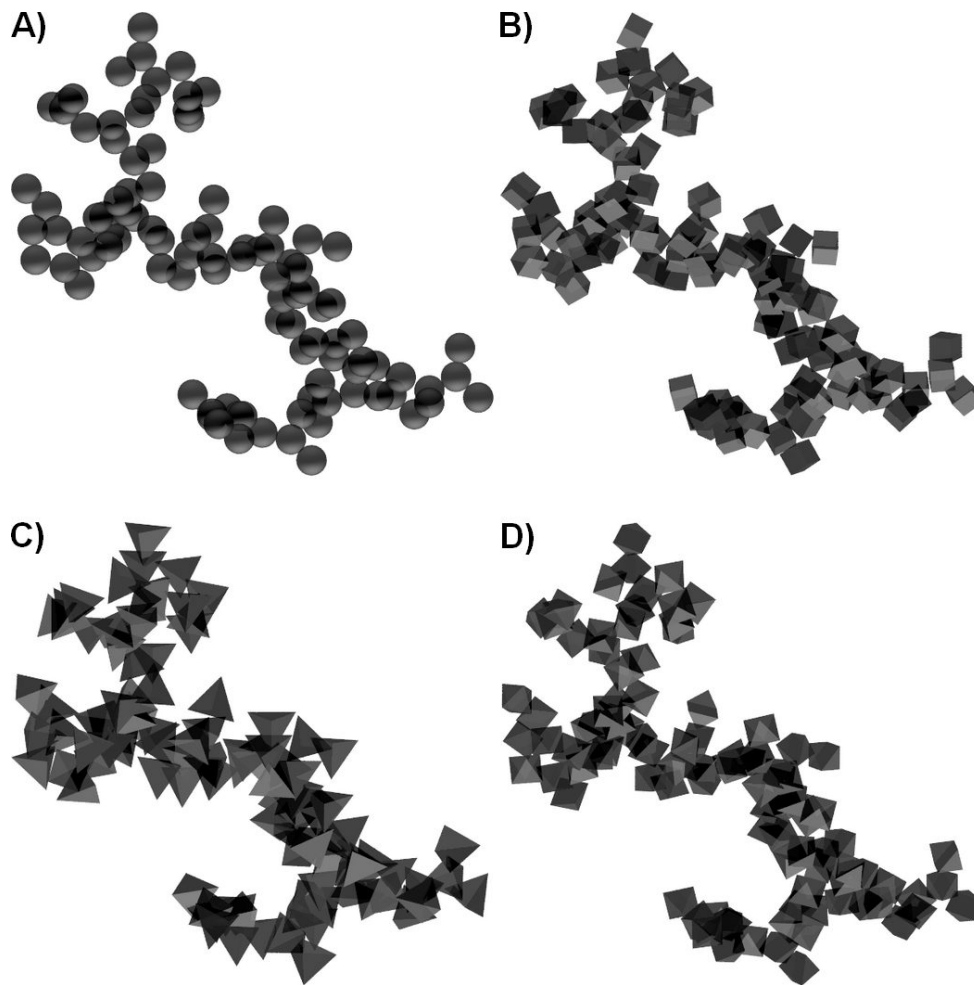


Figure 2: Sample fractal-like aggregate models composed of  $N_p = 100$ : A) spherical, B) cubical, C) tetrahedral, D) octahedral primary particles.

changed carelessly. The least significant absorption error  $C_{abs}$  was observed for the octahedral geometry. This was expected because it resembles the classic, spherical primary particle model. The relative scattering error  $\delta C_{sca}$  was much lower in every case. Furthermore, the value of the scattering cross section  $C_{sca}$  is about two orders of magnitude lower than the value of the absorption cross section  $C_{abs}$ . Therefore, it does not contribute to the extinction cross section  $C_{ext}$  significantly. The scattering diagrams are presented in Fig. 3. They are barely affected by the shape of the investigated model. This proves that, providing that primary particles are small (e.g.  $r_p = 15nm$ ), when scattering diagrams or the asymmetry parameter  $g$  are investigated, even complex particle shapes can be replaced with simple spherules.

### 3. SIMULATION RESULTS - AGGREGATES

In the next part of the study, due to the fact that the absorption cross section  $C_{abs}$  is the dominant component of the extinction cross section  $C_{ext}$  (even for large aggregates), only the second parameter, i.e.  $C_{ext}$ , was investigated. The relative extinction error  $C_{ext}$  for aggregates composed of a different number of primary particles  $N_p$  are presented in Fig. 6, Fig. 7 and Fig. 8. Once again, the tetrahedral model turns out to be most erroneous one, regardless of the aggregate size  $N_p$ . However, its value is much smaller than in the previous study and diminishes slightly along with the number of primary particles  $N_p$ . This proves that, even when the diameter of the primary particle  $d$  is relatively small compared to the diameter of the aggregate, the

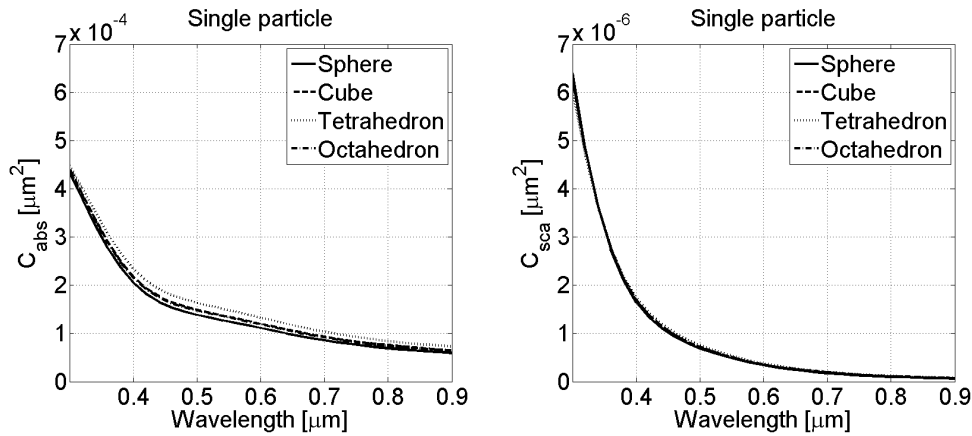


Figure 3: The comparison of the absorption cross section  $C_{abs}$  and the scattering cross section  $C_{sca}$  for different particle models.

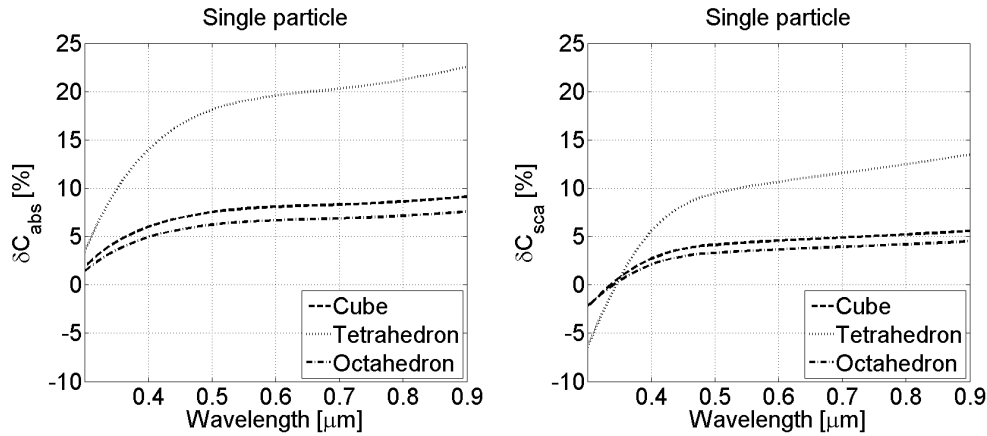


Figure 4: The comparison of the relative absorption error  $\delta C_{abs}$  and the relative scattering error  $\delta C_{sca}$  for different particle models.

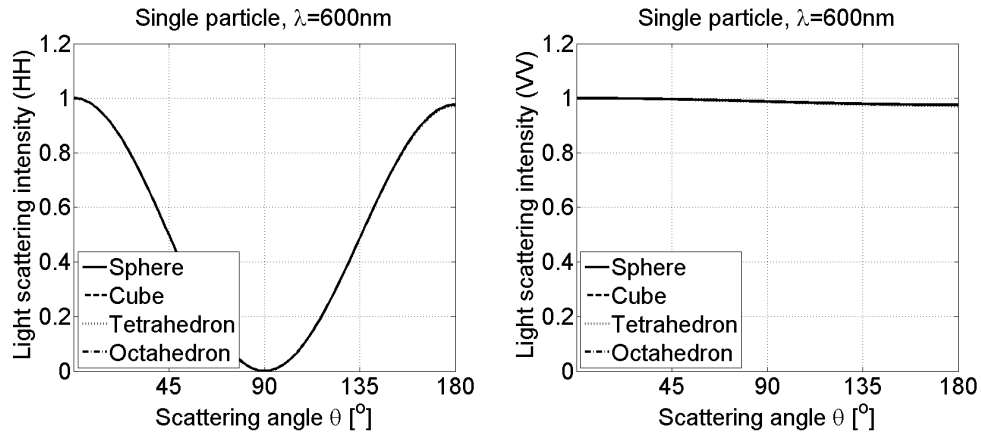


Figure 5: The comparison of the light scattering diagrams for different primary particle models. The incident wavelength was  $\lambda = 600nm$ .

complex particle shape should not be neglected. On the contrary, the changes in the scattering diagrams, and therefore, the asymmetry parameter  $g$ , are almost negligible, what is presented in Fig. 9.

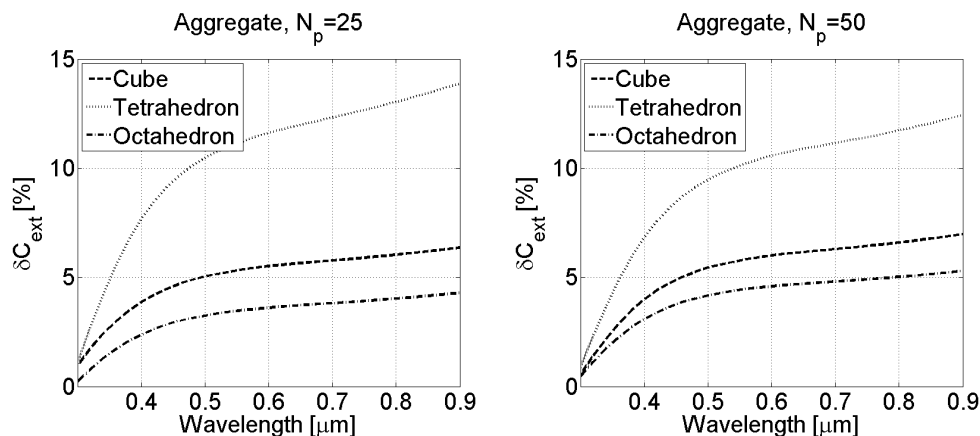


Figure 6: The comparison of the relative extinction error  $\delta C_{ext}$  for aggregates composed of  $N_p = 25$  and  $N_p = 50$  primary particles.

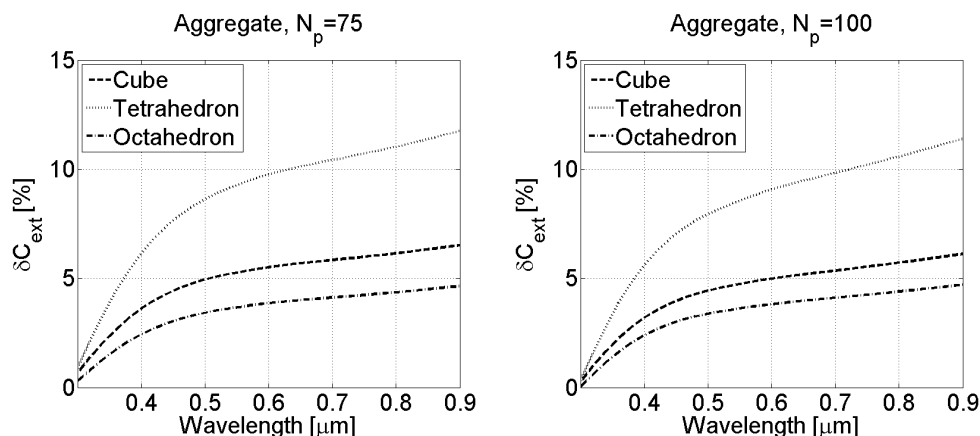


Figure 7: The comparison of the relative extinction error  $\delta C_{ext}$  for aggregates composed of  $N_p = 75$  and  $N_p = 100$  primary particles.

#### 4. CONCLUSIONS

In the study the impact of different primary particle models on the optical properties of fractal-like aggregates was investigated. Providing that primary particles are small and only scattering diagrams (or the asymmetry parameter  $g$ ) are required, even "extreme" shapes like tetrahedrons can be replaced with simple spherules. On the other hand, when the extinction cross section  $C_{ext}$  is needed, such simplifications can result in slightly erroneous data. Furthermore, even when fractal-like aggregates are large (e.g. they are composed of  $N_p = 300$  primary particles) such changes cannot be considered as non-existent.

#### 5. ACKNOWLEDGEMENT

I would like to acknowledge support of this research by the Polish Ministry of Science and Higher Education - K0401B50014 (0402/0013/15).

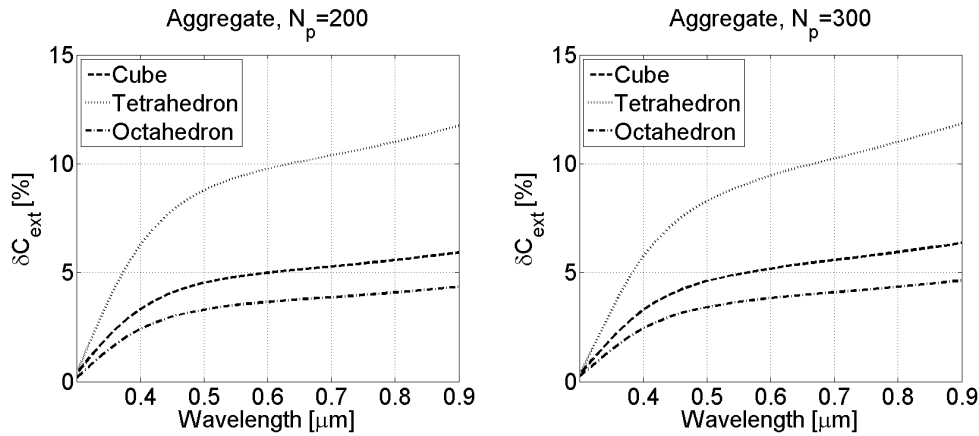


Figure 8: The comparison of the relative extinction error  $\delta C_{ext}$  for aggregates composed of  $N_p = 200$  and  $N_p = 300$  primary particles.

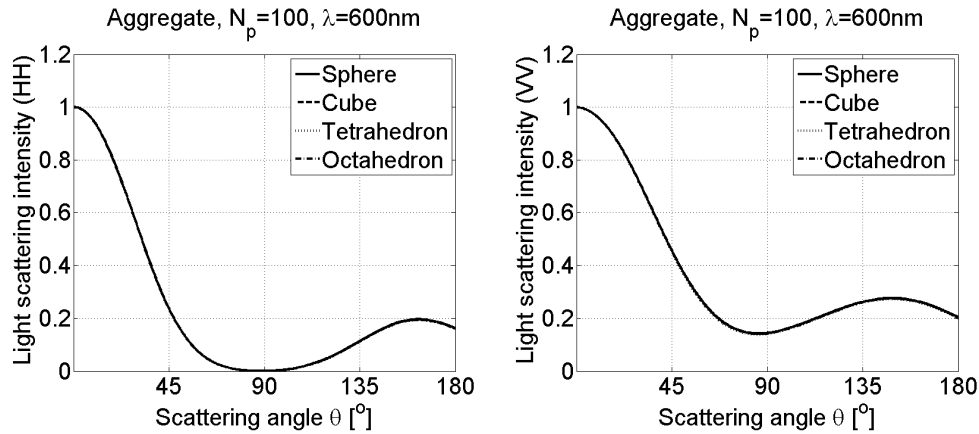


Figure 9: The comparison of the light scattering diagrams for aggregates composed of  $N_p = 100$  primary particles. The incident wavelength was  $\lambda = 600nm$ .

## REFERENCES

- [1] Mandelbrot, B., [*The Fractal Geometry of Nature*], W. H. Freeman and Co. (1982).
- [2] Sorensen, C. M., "Light scattering by fractal aggregates: A review," *Aerosol Science and Technology* **35**, 648–687 (2001).
- [3] Riefler, N., Stasio, S., and Wriedt, T., "Structural analysis of clusters using configurational and orientational averaging in light scattering analysis," *Journal of Quantitative Spectroscopy and Radiative Transfer* **89**, 323–342 (2004).
- [4] Brasil, A., Farias, T., Carvalho, G., and Koylu, U., "Numerical characterization of the morphology of aggregated particles," *Journal of Aerosol Science* **32**, 489–508 (2001).
- [5] Mackowski, D. and Mishchenko, M., "A multiple sphere t-matrix fortran code for use on parallel computer clusters," *Journal of Quantitative Spectroscopy and Radiative Transfer* **112**, 2182–2192 (2011).
- [6] Bahadur, J., Mazumder, S., Sen, D., and Ramanathan, S., "Evolution of a fractal system with conserved order parameter under thermal annealing," *Journal of Physics: Condensed Matter* **22**, doi:10.1088/0953-8984/22/19/195107 (2010).
- [7] Nel, A., Xia, T., Maedler, L., and Li, N., "Toxic potential of materials at the nanolevel," *Science* **311**, 622–627 (2006).

- [8] Bond, T., "Spectral dependence of visible light absorption by carbonaceous particles emitted from coal combustion," *Geophysical Research Letters* **28**, 4075–4078 (2001).
- [9] Bond, T. and Bergstrom, R., "Light absorption by carbonaceous particles: An investigative review," *Aerosol Science and Technology* **40**, 27–67 (2006).
- [10] Chang, H. and Charalampopoulos, T., "Determination of the wavelength dependence of refractive indices of flame soot," *Proceedings: Mathematical and Physical Sciences* **430**, 577–591 (1990).
- [11] Filippov, A., Zurita, M., and Rosner, D., "Fractal-like aggregates: Relation between morphology and physical properties," *Journal of Colloid and Interface Science* **229**, 261–273 (2000).
- [12] Filippov, A., "Drag and torque on clusters of  $n$  arbitrary spheres at low Reynolds number," *Journal of Colloid and Interface Science* **229**, 184–195 (2000).
- [13] Mroczka, J., "The cognitive process in metrology," *Measurement* **46**, 2896–2907 (2013).
- [14] Skorupski, K., Mroczka, J., Wriedt, T., and Riefler, N., "A fast and accurate implementation of tunable algorithms used for generation of fractal-like aggregate models," *Physica A: Statistical Mechanics and its Applications* **404**, 106–117 (2014).
- [15] Poppel, L. L., Friedrich, H., Spinsby, J., Chung, S. H., Seinfeld, J. H., and Buseck, P. R., "Electron tomography of nanoparticle clusters: Implications for atmospheric lifetimes and radiative forcing of soot," *Geophysical Research Letters* **32**, doi:10.1029/2005GL024461 (2005).
- [16] Katrinak, K., Rez, P., Perkes, P., and Buseck, P., "Fractal geometry of carbonaceous aggregates from an urban aerosol," *Environmental Science and Technology* **27**, 539–547 (1993).
- [17] Mroczka, J. and Szczuczynski, D., "Inverse problems formulated in terms of first-kind fredholm integral equations in indirect measurements," *Metrology and Measurement Systems* **16**, 333–357 (2009).
- [18] Mroczka, J. and Szczuczynski, D., "Improved regularized solution of the inverse problem in turbidimetric measurements," *Applied Optics* **5**, 4591 (2010).
- [19] Mroczka, J. and Szczuczynski, D., "Simulation research on improved regularized solution of the inverse problem in spectral extinction measurements," *Applied Optics* **51**, 1715–1723 (2012).
- [20] Mroczka, J. and Szczuczynski, D., "Improved technique of retrieving particle size distribution from angular scattering measurements," *Journal of Quantitative Spectroscopy and Radiative Transfer* **129**, 48–59 (2013).
- [21] Mroczka, J., Wozniak, M., and Onofri, F. R. A., "Algorithms and methods for analysis of the optical structure factor of fractal aggregates," *Metrology and Measurements Systems* **19**, 459–470 (2012).
- [22] Wozniak, M., Onofri, F. R. A., Barbosa, S., Yon, J., and Mroczka, J., "Comparison of methods to derive morphological parameters of multi-fractal samples of particle aggregates from TEM images," *Journal of Aerosol Science* **47**, 12–26 (2012).
- [23] Czerwinski, M., Mroczka, J., Girasole, T., Gouesbet, G., and Grehan, G., "Light-transmittance predictions under multiple-light-scattering conditions. I. direct problem: hybrid-method approximation," *Applied Optics* **40**, 1514–1524 (2001).
- [24] Czerwinski, M., Mroczka, J., Girasole, T., Gouesbet, G., and Grehan, G., "Light-transmittance predictions under multiple-light-scattering conditions. II. inverse problem: particle size determination," *Applied Optics* **40**, 1525–1531 (2001).
- [25] Heintzenberg, J., "Fine particles in the global troposphere: A review," *Tellus* **41B**, 149–160 (1989).
- [26] Wriedt, T., Hellmers, J., Eremina, E., and Schuh, R., "Light scattering by single erythrocyte: Comparison of different methods," *Journal of Quantitative Spectroscopy and Radiative Transfer* **100**, 444–456 (2006).
- [27] Nilsson, A., Alsholm, P., Karlsson, A., and Andersson-Engels, S., "T-matrix computations of light scattering by red blood cells," *Applied Optics* **37**, 2735–2748 (1998).
- [28] Mroczka, J. and Wysoczanski, D., "Plane-wave and gaussian-beam scattering on an infinite cylinder," *Optical Engineering* **39**, 736–770 (2000).
- [29] Girasole, T., Gouesbet, G., Grehan, G., Toulouzan, J. L., Mroczka, J., Ren, K., and Wysoczanski, D., "Cylindrical fibre orientation analysis by light scattering. part II: Experimental aspects," *Particle and Particle Systems Characterization* **14**, 211–218 (1997).
- [30] Girasole, T., Bultynck, H., Gouesbet, G., Grehan, G., Meur, F. L., Toulouzan, J. L., Mroczka, J., and Wysoczanski, D., "Cylindrical fibre orientation analysis by light scattering. part I: Numerical aspects," *Particle and Particle Systems Characterization* **14**, 163–174 (1997).

- [31] Girasole, T., Toulouzan, J. L., Mroczka, J., and Wysoczanski, D., "Fiber orientation and concentration analysis by light scattering: Experimental setup and diagnosis," *Review of Scientific Instruments* **68**, 2805–2811 (1997).
- [32] Swirniak, G., Glomb, G., and Mroczka, J., "Inverse analysis of light scattered at a small angle for characterization of a transparent dielectric fiber," *Applied Optics* **53**, 7103–7111 (2014).
- [33] Swirniak, G., Glomb, G., and Mroczka, J., "Inverse analysis of the rainbow for the case of low-coherent incident light to determine the diameter of a glass fiber," *Applied Optics* **53**, 4239–4247 (2014).
- [34] Skorupski, K., Mroczka, J., Riefler, N., Oltmann, H., Will, S., and Wriedt, T., "Impact of morphological parameters onto simulated light scattering patterns," *Journal of Quantitative Spectroscopy and Radiative Transfer* **119**, 53–66 (2013).
- [35] Skorupski, K., Mroczka, J., Riefler, N., Oltmann, H., Will, S., and Wriedt, T., "Effect of the necking phenomenon on the optical properties of soot particles," *Journal of Quantitative Spectroscopy and Radiative Transfer* **141**, 40–48 (2014).
- [36] Yurkin, M. and Hoekstra, A., "The discrete dipole approximation: An overview and recent developments," *Journal of Quantitative Spectroscopy and Radiative Transfer* **106**, 558–589 (2007).
- [37] Yurkin, M. and Hoekstra, A., "The discrete-dipole-approximation code ADDA: Capabilities and known limitations," *Journal of Quantitative Spectroscopy and Radiative Transfer* **112**, 2234–2247 (2011).